



OPEN

A new class of fluorescent-dots: long luminescent lifetime bio-dots self-assembled from DNA at low temperatures

Chun Xian Guo^{1,2}, Jiale Xie^{1,2}, Bin Wang^{1,2}, Xinting Zheng^{1,2}, Hong Bin Yang³ & Chang Ming Li^{1,2,3}

¹Institute for Clean Energy & Advanced Materials, Southwest University, Chongqing 400715, P. R. China, ²Chongqing Key Laboratory for Advanced Materials and Technologies of Clean Energies, Chongqing 400715, P. R. China, ³School of Chemical and Biomedical Engineering, Nanyang Technological University, 637457, Singapore.

Received

11 June 2013

Accepted

30 September 2013

Published

16 October 2013

Correspondence and requests for materials should be addressed to C.M.L. (ecmli@swu.edu.cn)

Quantum-dots (QDs) have fuelled up intensive research efforts over the past two decades. Nevertheless, currently developed two classes of fluorescent QDs, colloidal semiconductor QDs and carbonaceous QDs suffer from either toxicity or short luminescence lifetime. Here, we report a new class of fluorescent bio-dots that are derived from DNA via self-assembly at low temperatures down to 80 °C, which has an optical bandgap of 3.4 eV, and in particular possesses strong photoluminescence with a much longer luminescence lifetime ($\tau_1 = 10.44$ ns) than the carbonaceous QDs ($\tau_1 < 0.5$ ns). It is discovered that it is the interactions of base pair cytosines with each other to form sp^2 carbon-like centers as luminescence centers or chromophores for the photoluminescence. The use of bio-dots in cell imaging with strong photoluminescence signal and good biocompatibility demonstrates great potentials of broad biological and optoelectronic applications.

Quantum-dots (QDs) and their applications have become one of the fastest moving and most exciting nanotechnologies over the past two decades^{1,2}. Currently two classes of fluorescent QDs, colloidal semiconductor QDs and carbonaceous QDs, have fuelled up intensive research efforts. Colloidal semiconductor QDs offer a long luminescence lifetime ($\tau_1 > 10$ ns) for various biological and optoelectronic applications^{3–9}, but their toxicity or the use of hazardous solvents/ligands become the main blockage for broad biological applications^{10–13}. Carbonaceous QDs are toxic-free^{14–19}, however, their short luminescence lifetime, for example, $\tau_1 < 0.50$ ns for graphene QDs²⁰ significantly limits the uses in biology because a fluorescent material with a short luminescence lifetime may suffer interferences from some biological molecules that always have short fluorescent lifetimes. Here, we report a new class of fluorescent dots, namely bio-dots that are derived from DNA via self-assembly at relatively low temperatures even down to 80 °C, which has an optical bandgap of 3.4 eV and possesses strong photoluminescence with a much longer luminescence lifetime ($\tau_1 = 10.44$ ns) than the carbonaceous QDs while retaining partial structures of DNA including phosphate groups on the backbone to have high biocompatibility. The bio-dots are further demonstrated their application in cell imaging.

Results

Preparation and optical properties of bio-dots. Preparation of the bio-dots is schematically shown in Fig. 1a. Double-strand DNA was water-dissolved in a sealed container at temperature of 80 °C or above for 12 hours or longer and become single strand DNA firstly, followed by self-assembly and converting to bio-dots. Under illumination at 365 nm, the bio-dots have a bright blue photoluminescence (PL) while no PL is observed for DNA (Fig. 1b), which rules out the possibility of PL from DNA. With respect to the adsorption, DNA has a maximum absorption peak at 260 nm, which is attributed to the presence of delocalised π electron from heterocyclic rings of purines and pyrimidines in DNA²¹. The bio-dots have two absorption peaks, of which one is located as same as DNA while another one is in the range of 300 to 400 nm (Fig. 1c), indicating that they well retain the heterocyclic rings of DNA but with a different molecular structure. Fig. 1c displays bio-dots' emission spectra under different excitation wavelengths (λ_{ex}) ranging from 350 to 410 nm. As the excitation

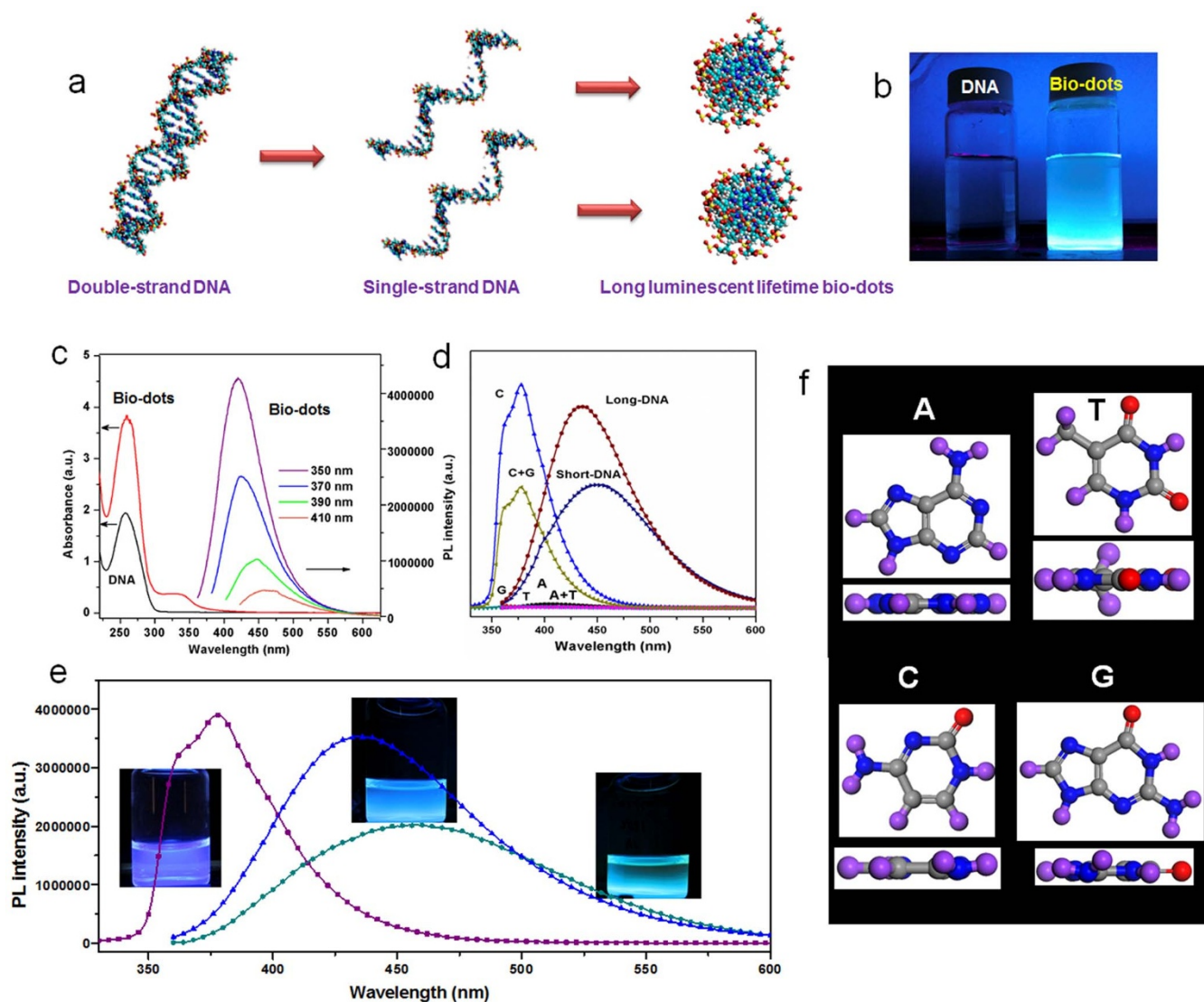


Figure 1 | Optical properties of bio-dots. (a), Scheme showing the formation process of bio-dots. (b), DNA and bio-dots aqueous solutions under illumination at 365 nm. (c), UV-vis absorption of DNA and bio-dots and PL emission spectra of bio-dots. (d), Bio-dots derived from different components. (e), Three kinds of bio-dots with different PL wavelengths. (f), Molecular structure of base pairs of DNA: carbon (grey color), nitrogen (blue color), oxygen (red color) and hydrogen (purple color).

wavelength increases, the emission peak position of the bio-dots displays a red-shift behavior and the emission peak intensity decreases, exhibiting excitation-dependent PL emission.

We measured PLs of different bio-dots prepared from base pairs of adenine (A), thymine (T), cytosine (C), and guanine (G), and also same sequenced DNA fragments with different lengths termed as short-DNA and long-DNA, respectively. The bio-dots prepared from short- and long-DNA are called as short- and long-DNA bio-dots, respectively. It is found that the bio-dots made from DNAs containing only cytosine base pairs can generate good PL, thus indicating that cytosine plays a critical role in PL generation. Comparison of the molecular structures of the four types of base pairs (Fig. 1f) reveals that cytosine comprises the structure of pyrimidine while without methyl group, leading to all the atoms locating in a same plane. This unique cytosine molecular structure might be beneficial to the formation of luminescence centers or chromophores through self-interactions for the bio-dots. Bio-dots derived from DNAs with different lengths display good PLs but with differences in peak wavelength and intensity (Fig. 1d). Effects of synthesis temperature on PL behavior of bio-dots were studied with results given in Fig. S1 and S2,

discovering that a temperature as low as 80°C can well produce bio-dots with good PL. The PL intensity gradually increases and the peak wavelength shifts towards longer wavelength with increase of the temperature up to 140°C. Treatment time is also found to have effect on the PL intensity, which increases with increase of the time up to 12 h and then keeping almost constant. Thus, by controlling the preparation conditions, bio-dots can be tailored to have different PL behaviors corresponding to different PL peak wavelengths and intensities within the near UV region (Fig. 1e). The bio-dots were tested under continuous excitation for 2 h and their PL intensity does not have any obvious change observed, indicating good photostability. In aqueous solution with pH ranging from 5 to 9, the PL intensity has no obvious change, suggesting its pH independent characteristic.

Structure and component characterizations of the bio-dots. The formation process of bio-dots was monitored by AFM. To clearly understand the formation process, long-DNA was used. Fig. 2a shows that the original DNA has a linear long chain. The product obtained with temperature treatment for half an hour contains a

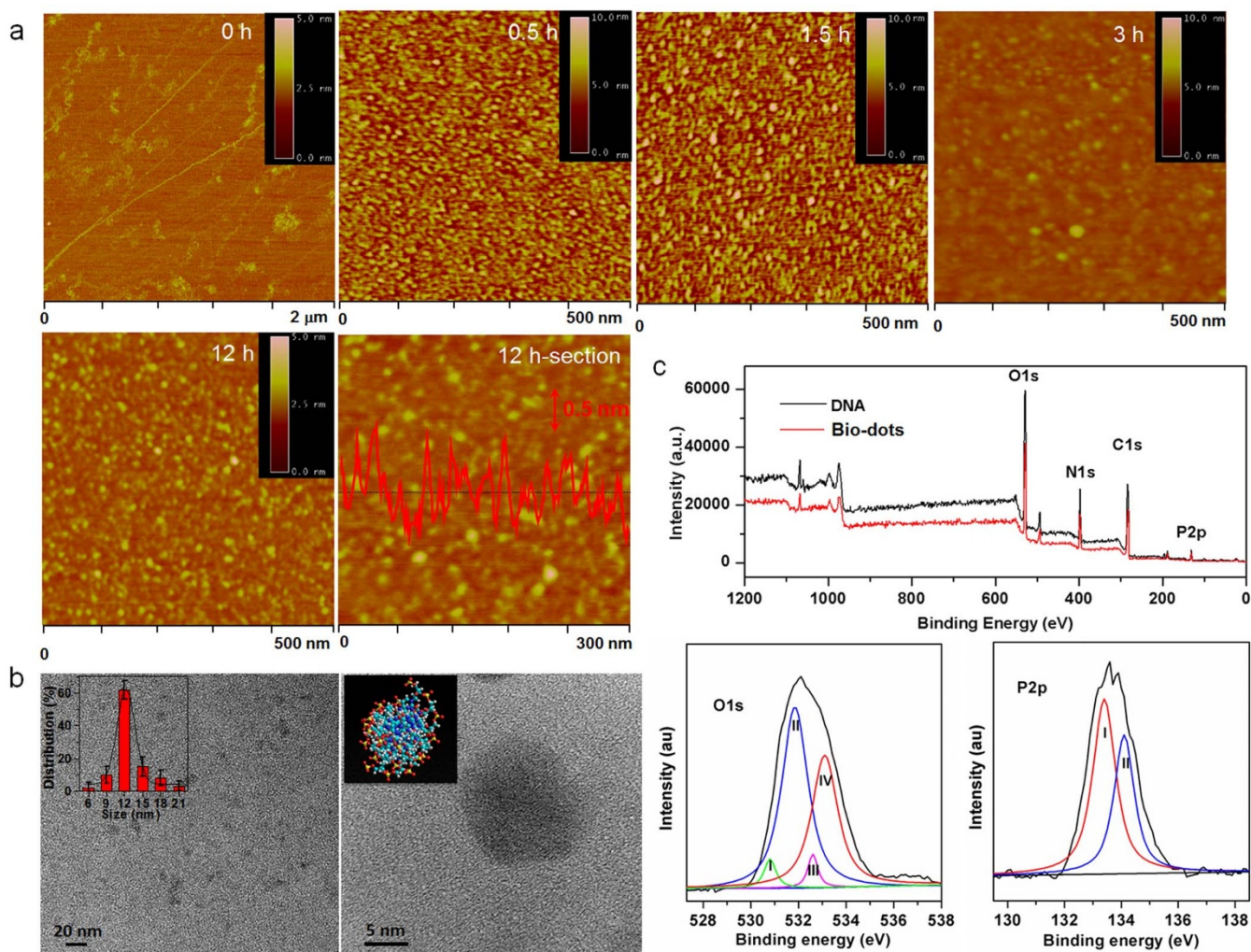


Figure 2 | Structure and component characterizations of the bio-dots. (a) AFM characterization showing formation process of the bio-dots: DNA temperature treated with different times and corresponding section analysis. (b) TEM images of bio-dots and the inset displaying size distribution. (c) Wide XPS survey of DNA and bio-dots, and high-resolution XPS O1s and P2p spectra of bio-dots.

mixture of bio-dots and DNA fragments, and the ratio of bio-dot/DNA fragment increases with the increase of the treatment time. When the treatment time is 12 hours or longer, the product only composes of bio-dots with an average roughness of around 1 nm, as measured from section analysis of the AFM high profile. The AFM characterization suggests that the formation of bio-dots is a time-evolved process, gradually changing from a chain fragment to a bio-dot via self-assembly. TEM image of short-DNA bio-dots in Fig. 2b reveals that they well separate from each other. From a count of 250 bio-dots, the corresponding particle size distribution histogram (inset of Fig. 2b) tells that the bio-dots have an average size of ~ 12 nm. The shape of bio-dots is further evidenced by the high magnification TEM image. Different from that of short-DNA bio-dots, long-DNA bio-dots have relatively larger sizes mainly around 25 nm.

Composition and element analysis of the bio-dots were conducted by XPS. The wide scan XPS spectra in Fig. 2c show four peaks at 133.5, 284.0, 400.0, and 530.6 eV, which are attributed to P2p, C1s, N1s and O1s respectively for both DNA²² and bio-dots, evidencing that the bio-dots composition is close to that of DNA. The high-resolution O1s spectrum of the bio-dots also display four peaks at 530.8, 532.0, 532.6 and 533.2 eV, which are attributed to the PO_4^{1-} , O=C, O-N²³ and O-C bands, respectively. It is known that DNA contains PO_4^{1-} , O=C and O-C while lacking O-N²². The O-N should be generated during the preparation of bio-dots. The high-resolution P2p spectrum of bio-dots exhibits two peaks at 133.2 and

134.3 eV, which are attributed to the 2p_{3/2} and 2p_{1/2} bands²², respectively, and are identical to that of DNA. This suggests that the PO_4^{1-} groups on the backbone of DNA are well retained in the bio-dots. Therefore, it is very likely that the O-N band of bio-dots comes from the interaction between base pairs of DNA instead of base pair and PO_4^{1-} .

Optical properties of bio-dots and the practicality for cell imaging.

The luminescence decay profile of the bio-dots in Fig. 3a was obtained by using a time correlated single photon counting technique with recording the bio-dots transitions at 465 nm emission that was excited at 370 nm. The luminescence lifetime data are very well fitted to an exponential function and the fitting results generated from iterative reconvolution of the decay with the instrument response function are given in the inset of Fig. 3a, indicating that the observed lifetime (τ_1) is 10.44 ns with a correction of 0.937. The lifetime is much longer than that of carbonaceous dots ($\tau_1 < 0.5$ ns)²⁰. The mechanism for the long luminescence lifetime for the bio-dots is not clear yet and further study is needed. The optical bandgap of the DNA bio-dots calculated from Uv-vis adsorption data in Fig. 3b is 3.4 eV.

The formation mechanism and the PL behavior of the bio-dots could be explained from the material characterization results. It is very likely that the interaction between base pairs of DNA results in a new band, while well retaining groups on the backbone (Fig. 2c). In

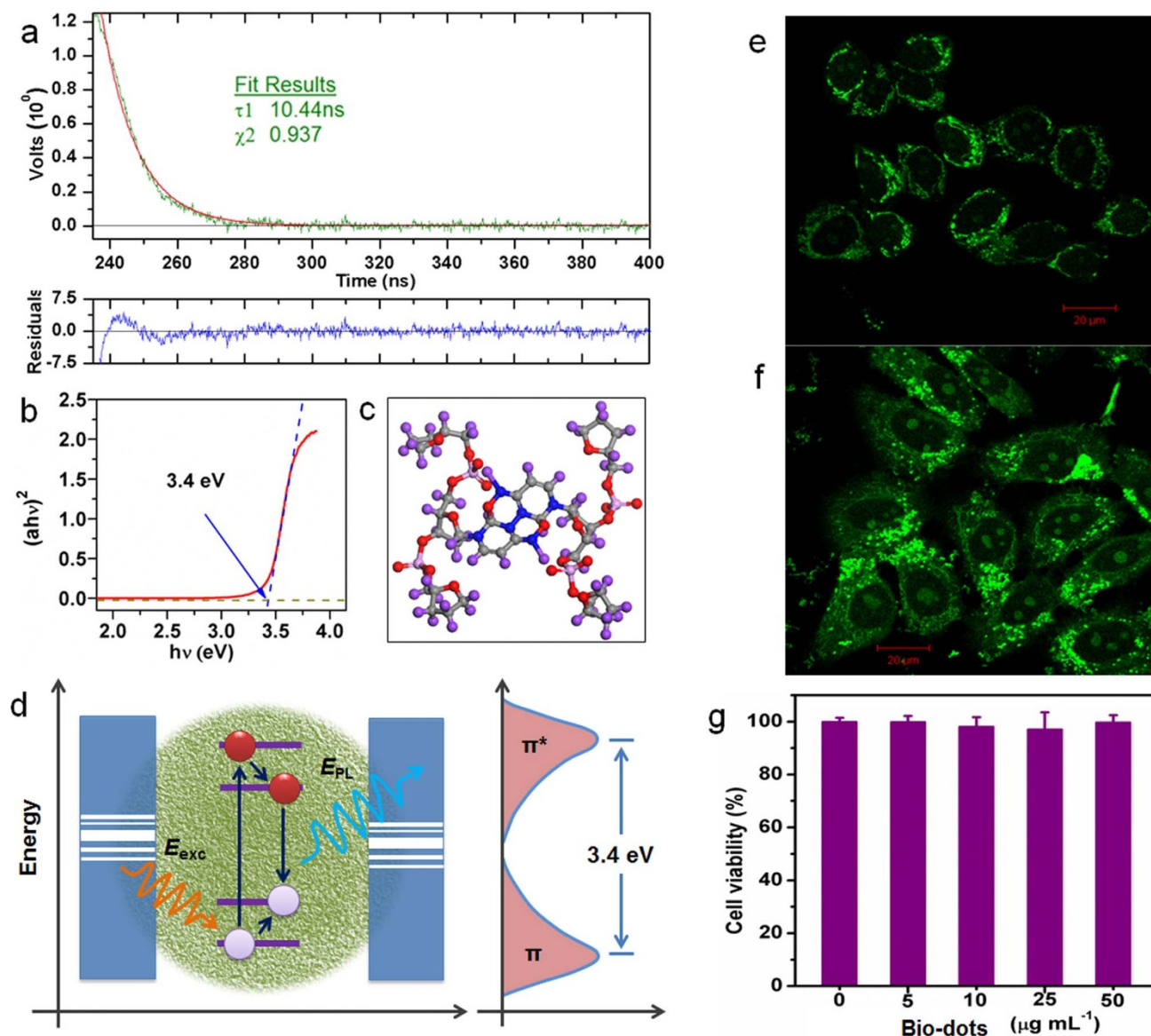


Figure 3 | Optical properties of bio-dots and the practicality for cell imaging. (a) Resolved photoluminescence (TRPL) decay profile of bio-dots recorded at room temperature. The inset shows the parameter generated by the exponential fitting of the TRPL decay profile. (b) Optical bandgap of the bio-dots obtained from Uv-vis adsorption. (c) Scheme showing a sp^2 carbon-like center of bio-dots formed between the interaction of two cytosine molecules. (d) Representative band structure of bio-dots. The energy levels are quantized with optical bandgap as observed from PL and Uv-vis adsorption characterization results. A photoinduced electron-hole pair recombining radiatively is described. (e) Fluorescent image of cell incubation with long-DNA bio-dots (concentration of $12.5 \mu\text{g mL}^{-1}$). (f) Fluorescent image of cell incubation with short-DNA bio-dots (concentration of $12.5 \mu\text{g mL}^{-1}$). (g) Biocompatibility testing of the bio-dots.

particular, cytosine containing oxygen groups has the basic structure with all the atoms locating in a same plane, and its inter-molecule interaction could form sp^2 carbon-like centers (Fig. 1d and 1f). A possible chemical reaction occurs between oxygen groups and amine groups on different cytosine bases to form new O–N bonds, about which a computation work was conducted with results given in Fig. 3c. It is worthy of a note that stacking of the aromatic cytosine base pairs to form sp^2 carbon-like center cannot be excluded. On the other hand, the highly hydrophilic PO_4^{1-} groups on the backbone should dunk in aqueous solution, thus locating outside the cytosine-derived sp^2 carbon-like centers and further wrapping them to form shaped bio-dots. The bio-dots have an optical bandgap of ~ 3.4 eV (Fig. 3b), which should be resulted from π and π^* states of the cytosine derived sp^2 carbon-like centers that lie within the bandgap of other parts of bio-dots such as PO_4^{1-} groups on the backbone. The

cytosine-derived sp^2 carbon-like centers should be the luminescence centers or chromophores to play a critical role, in which a structure allows radiative recombination of the trap carriers for a generic photophysical mechanism (Fig. 3d). To better understand the PL mechanism of the bio-dots, we compare PL behavior of the bio-dots with that of carbon quantum dots. It has been realized carbon quantum dots contain a mixture of sp^2 clusters and sp^3 carbon although no direct observation of sp^2 domains has been reported²⁴. The PL behavior of carbon quantum dots is generally considered to be determined by the π and π^* electronic levels of the sp^2 clusters that lie within the bandgap of s and s^* states of the sp^3 matrix^{24,25}. Considering the similar structure of the bio-dots as that of carbon quantum dots, the PL mechanism of carbon quantum dots provides an indirect way to support the PL mechanism of the bio-dots proposed above. Although both of these two materials have PL, the



bio-dots have unique advantages of much longer lifetime (τ_1 of >10 ns vs. <0.5 ns) and lower preparation temperature (as lower as 80°C vs. $>180^\circ\text{C}$). By selecting Rhodamine 6G as a standard, the DNA bio-dots under excitation at 350 nm have a PL quantum yield of 3.65%, which is comparable to that of carbonaceous QDs such as graphene QDs (2.29%) as reported²⁶.

We evaluated the application of the bio-dots in cell imaging by using human breast cancer MCF7 cells as a sample. Long- and short-DNA bio-dots with similar PL behavior but different sizes are used. As shown in Fig. 3e and 3f, both of the two kinds of bio-dots provide good fluorescent signal for cell imaging, and they can be located in the cell membrane and cytoplasm. These bio-dots are very likely internalized into the cells through cell membrane via endocytosis. A control experiment for fluorescent images of cells without incubation of bio-dots in Fig. S3 shows that negligible endogenous fluorescence and no obvious autofluorescence from the nucleolus are observed under the same imaging conditions. It is also noted that the bio-dots have a much higher distribution on some parts of cells, about which further study is needed. An interesting phenomenon is that the inner parts of cells have a much brighter fluorescent signal for cells incubations with short-DNA bio-dots than that with long-DNA bio-dots. A possible reason is that short-DNA bio-dots have a much higher molar concentration than the long-DNA bio-dots although they are used with the same mass concentration ($12.5 \mu\text{g mL}^{-1}$). The main difference between short- and long-DNA bio-dots is the size, thus it is also possible that cells allow bio-dots with small size penetrating while preventing those with larger sizes. Exact reasons for cells labelled with short-DNA bio-dots showing brighter fluorescent signal are not clear yet and further studies are needed. The cytotoxicity of the bio-dots was evaluated using MTT viability assay, and the average cell viability was greater than 98% at all these tested bio-dots concentrations ranging from 0 to $50 \mu\text{g mL}^{-1}$. Even at a concentration up to $65 \mu\text{g mL}^{-1}$, the average cell viability was still greater than 90%, which is comparable and even better than that for carbonaceous QDs at similar conditions^{20,25}. Cell proliferation at these dosages as the exposure time increases up to 24 hours was not affected. These results reveal that the bio-dots are very biocompatible.

Discussion

In brief, here we report a new class of fluorescent dots, bio-dots derived from DNA via self-assembly. We discover that the interaction of base pair cytosines with each other forms sp^2 carbon-like centers, which behave as the luminescence centers or chromophores for the photoluminescence. The bio-dots have a long luminescence lifetime (τ_1) of 10.44 ns, which is much longer than that of other organic quantum dots such as graphene quantum dots ($\tau_1 < 0.50$ ns). The bio-dots demonstrate an application in cell imaging with good photoluminescence signal and high biocompatibility. It is believed that these bio-dots could also offer great potential applications in other biological applications and optoelectronics.

Methods

Preparation of bio-dots. Deoxyribonucleic acid sodium salt from salmon testes (long-DNA, approximately 2000 bp) and Deoxyribonucleic acid, low molecular weight, from salmon sperm (short-DNA, approximately 200 bp) were purchased from Sigma-Aldrich. Base pairs of adenine (A), thymine (T), cytosine (C), guanine (G), and all other chemicals were purchased from Sigma-Aldrich and used as received.

DNA was dissolved in double deionized water with different concentrations (10 to 50 mg mL^{-1}) and the solution was stirred at 300 rpm for half an hour. Then the solution was put into a sealed glass bottle for temperature lower than 120°C or into a stainless steel autoclave for temperature higher than 120°C . The heating temperature range is from 80 to 180°C and the treatment time is from half an hour to 24 hours. To prepare bio-dots from base pairs, the saturated aqueous solutions of base pairs were used with all other preparation procedures the same as those for bio-dots from DNA.

Material characterizations. The formation process of bio-dots was characterized by atomic force microscopy (AFM, Nanoman, Veeco, Santa Barbara, CA) using tapping

mode and operating in air. The morphology and structure of the bio-dots were investigated by HRTEM (JEM-2100F, Japan). Corresponding particle size distribution histogram was plotted from a count of 250 bio-dots. The adsorption profile was obtained with a Shimadzu UV-2450 spectrophotometer. Photoluminescence (PL) spectra were recorded using an Aminco Bowman II luminescence spectrometer (Thermo Electron, USA). XPS characterizations were performed on a PHI Quantera x-ray photoelectron spectrometer with a chamber pressure of 5×10^{-9} torr and an Al cathode as the X-ray source. Time resolved photoluminescence was recorded using a time-correlated single photon counting technique with an Edinburgh spectrometer (Edinburgh FLSP-920) using picosecond laser diodes as the source of excitation. The molecular structures were generated by using Materials studio 5.5 with the help of DMol3 and GGA-PW91. The set of convergence thresholds for DMol3 is 'Fine' with values of the convergence thresholds as follows: Energy (Hartree) of 1×10^{-5} , Max. force (Hartree angstrom $^{-1}$) of 0.002, and Max. displacement (angstrom $^{-1}$) of 0.005. With these parameters, the program ran until the structure was optimized.

Cell imaging and cytotoxicity evaluation. HER2 over-expressing human breast cancer MCF7 (MCF7/HER2) cells were cultured with Dulbecco's Modified Eagle's Medium (DMEM) (PAA Laboratories) supplemented with 10% heat inactivated FBS, 50 U mL^{-1} penicillin/streptomycin (Gibco) and 0.5 mg mL^{-1} G418 (PAA Laboratories). The cells were grown in a humidified incubator at 37°C with 5.0% CO_2 . Cells were seeded at a density of 1×10^4 cells cm^{-2} onto poly-L-lysine (0.1 mg mL^{-1}) coated coverslips for cell attachment. 1×10^4 cells were plated in each well of a 4 well sterile chamber slides. After overnight culture, different concentrations of DNA bio-dots were added in culture medium and incubated in regular cell culture conditions. After 4 hours of culture, cell medium containing bio-dots was removed from the cells and washed several times with phosphate buffered saline (PBS) (pH 7.4). Fluorescence images were acquired using a Zeiss LSM 510 Meta confocal microscope at excitation laser wavelength of 405 nm with a corresponding default fluorescence emission filters on the microscope. For cytotoxicity evaluation, the cell was incubated with different concentrations of bio-dots for 24 hours. Then cells were washed gently with phosphate buffered saline (PBS) (pH 7.4). Then 3-(4,5-dimethyl-2-thiazolyl)-2,5-diphenyltetrazolium bromide (MTT) was added and incubated for 4h and then removed. Dimethyl sulfoxide was added the cells and incubated for additional 5 min at room temperature. Optical densities were measured at 570 nm in a Tecan Infinite microplate reader (Mannedorf, Switzerland).

- Galland, C. *et al.* Lifetime blinking in nonblinking nanocrystal quantum dots. *Nat. Commun.* **3**, 908 (2012).
- Michalet, X. *et al.* Quantum dots for live cells, in vivo imaging, and diagnostics. *Science* **307**, 538–544 (2005).
- Stuerzenbaum, S. R. *et al.* Biosynthesis of luminescent quantum dots in an earthworm. *Nat. Nanotechnol.* **8**, 57–60 (2013).
- Ropp, C. *et al.* Nanoscale imaging and spontaneous emission control with a single nano-positioned quantum dot. *Nat. Commun.* **4**, 1447 (2013).
- Sau, J. D. & Das Sarma, S. Realizing a robust practical Majorana chain in a quantum-dot-superconductor linear array. *Nat. Commun.* **3**, 964 (2012).
- Xiong, L. Q., Shuhendler, A. J. & Rao, J. H. Self-luminescing BRET-FRET near-infrared dots for in vivo lymph-node mapping and tumour imaging. *Nat. Commun.* **3**, 1193 (2012).
- Jin, Y. D., Jia, C. X., Huang, S. W., O'Donnell, M. & Gao, X. H. Multifunctional nanoparticles as coupled contrast agents. *Nat. Commun.* **1**, 41 (2010).
- Miller, T. A. *et al.* The mechanism of ultrafast structural switching in superionic copper (I) sulphide nanocrystals. *Nat. Commun.* **4**, 1369 (2013).
- Mohanty, N. *et al.* Nanotomy-based production of transferable and dispersible graphene nanostructures of controlled shape and size. *Nat. Commun.* **3**, 844 (2012).
- Guo, C. X., Dong, Y. Q., Yang, H. B. & Li, C. M. Graphene quantum dots as a green sensitizer to functionalize ZnO nanowire arrays on F-doped SnO_2 glass for enhanced photoelectrochemical water splitting. *Adv. Energy. Mater.* **3**, 997–1003 (2013).
- Lodahl, P. *et al.* Controlling the dynamics of spontaneous emission from quantum dots by photonic crystals. *Nature* **430**, 654–657 (2004).
- Auffan, M. *et al.* Towards a definition of inorganic nanoparticles from an environmental, health and safety perspective. *Nat. Nanotechnol.* **4**, 634–641 (2009).
- Hardman, R. A toxicologic review of quantum dots: Toxicity depends on physicochemical and environmental factors. *Environ. Health Persp.* **114**, 165–172 (2006).
- Lu, J., Yeo, P. S. E., Gan, C. K., Wu, P. & Loh, K. P. Transforming C-60 molecules into graphene quantum dots. *Nat. Nanotechnol.* **6**, 247–252 (2011).
- Baker, S. N. & Baker, G. A. Luminescent Carbon Nanodots: Emergent Nanolights. *Angew. Chem. Int. Ed.* **49**, 6726–6744 (2010).
- Zhu, S. *et al.* Surface Chemistry Routes to Modulate the Photoluminescence of Graphene Quantum Dots: From Fluorescence Mechanism to Up-Conversion Bioimaging Applications. *Adv. Funct. Mater.* **22**, 4732–4740 (2012).
- Liu, S. *et al.* Hydrothermal Treatment of Grass: A Low-Cost, Green Route to Nitrogen-Doped, Carbon-Rich, Photoluminescent Polymer Nanodots as an Effective Fluorescent Sensing Platform for Label-Free Detection of Cu(II) Ions. *Adv. Mater.* **24**, 2037–2041 (2012).



18. Li, H. *et al.* Water-Soluble Fluorescent Carbon Quantum Dots and Photocatalyst Design. *Angew. Chem. Int. Ed.* **49**, 4430–4434 (2010).
19. Sun, Y. P. *et al.* Quantum-sized carbon dots for bright and colorful photoluminescence. *J. Am. Chem. Soc.* **128**, 7756–7757 (2006).
20. Peng, J. *et al.* Graphene Quantum Dots Derived from Carbon Fibers. *Nano Lett.* **12**, 844–849 (2012).
21. Gallagher, S. Quantitation of DNA and RNA with Absorption and Fluorescence Spectroscopy. *Curr. Protoc. Protein Sci.* DOI:10.1002/0471140864.psa04ks52 (2008).
22. Majumder, S., Priyadarshini, M., Subudhi, U., Chainy, G. B. N. & Varma, S. X-ray photoelectron spectroscopic investigations of modifications in plasmid DNA after interaction with Hg nanoparticles. *Appl. Surf. Sci.* **256**, 438–442 (2009).
23. Olivares, O. *et al.* Electrochemical and XPS studies of decylamides of α -amino acids adsorption on carbon steel in acidic environment. *Appl. Surf. Sci.* **252**, 2894–2909 (2006).
24. Eda, G. *et al.* Blue Photoluminescence from Chemically Derived Graphene Oxide. *Adv. Mater.* **22**, 505–509 (2010).
25. Hsu, P. C., Shih, Z. Y., Lee, C. H. & Chang, H. T. Synthesis and analytical applications of photoluminescent carbon nanodots. *Green Chem.* **14**, 917–920 (2012).
26. Dong, Y. Q. *et al.* One-step and high yield simultaneous preparation of single- and multi-layer graphene quantum dots from CX-72 carbon black. *J. Mater. Chem.* **22**, 8764–8766 (2012).

Acknowledgements

This work was supported by Institute for Clean Energy & Advanced Materials (Southwest University, Chongqing, China), Chongqing Key Laboratory for Advanced Materials and

Technologies of Clean Energies, Start-up grant under SWU111071 from Southwest University, Chongqing Science and Technology Commission under cstc2012ghz90002, Chongqing Engineering Research Center for Rapid diagnosis of Dread Disease, and Chongqing development and reform commission and National Natural Scientific Fund (No. 21375108).

Author contributions

Experiments were designed by C.M.L. and C.X.G. Material characterizations were carried out by C.X.G. Computer simulation was done by C.X.G. and J.L.X. Cell imaging was performed by X.T.Z. The luminescence decay profile was recorded by H.B.Y. and adsorption profile was obtained with the help of B.W. The manuscript was written by C.M.L. and C.X.G.

Additional information

Supplementary information accompanies this paper at <http://www.nature.com/scientificreports>

Competing financial interests: The authors declare no competing financial interests.

How to cite this article: Guo, C.X. *et al.* A new class of fluorescent-dots: long luminescent lifetime bio-dots self-assembled from DNA at low temperatures. *Sci. Rep.* **3**, 2957; DOI:10.1038/srep02957 (2013).



This work is licensed under a Creative Commons Attribution-NonCommercial-NoDerivs 3.0 Unported license. To view a copy of this license, visit <http://creativecommons.org/licenses/by-nc-nd/3.0>